Open Access Full Text Article

ORIGINAL RESEARCH

Continuous quantitative measurement of the main bronchial dimensions and lung density in the lateral position by four-dimensional dynamic-ventilation CT in smokers and COPD patients

Yukihiro Nagatani,[1] Masayuki Hashimoto,[2] Norihisa Nitta,[1] Yasuhiko Oshio,[2] Tsuneo Yamashiro,[3] Shigetaka Sato,[1] Shinsuke Tsukagoshi,[4] Hiroshi Moriya,[5] Tatsuya Kimoto,[6] Tomoyuki Igarashi,[2] Noritoshi Ushio,[1] Akinaga Sonoda,[1] Hideji Otani,[1] Jun Hanaoka,[2] Kiyoshi Murata[1]

On behalf of investigators of the ACTIve Study Group

[1]Department of Radiology, Shiga University of Medical Science, Otsu, Shiga 520-2192, Japan; [2]Department of Surgery, Division of General Thoracic Surgery, Shiga University of Medical Science, Otsu, Shiga 520-2192, Japan; [3]Department of Radiology, Graduate School of Medical Science, University of the Ryukyus, Nishihara, Okinawa 903-0215, Japan; [4]CT System Division, Canon Medical Systems, Otawara, Tochigi 324-8550, Japan; [5]Department of Radiology, Ohara General Hospital, Fukushima, Fukushima 960-8611, Japan; [6]Healthcare IT Development Center, Canon Medical Systems, Otawara, Tochigi 324-8550, Japan

Correspondence: Tsuneo Yamashiro
Department of Radiology, Graduate School of Medical Science, University of the Ryukyus, 207 Uehara, Nishihara, Okinawa 903-0215, Japan
Tel +81 98 895 1162
Fax +81 98 895 1420
Email clatsune@yahoo.co.jp

Purpose: The purpose of this study was to measure changes in lung density and airway dimension in smokers in the lateral position using four-dimensional dynamic-ventilation computed tomography (CT) during free breathing and to evaluate their correlations with spirometric values.

Materials and methods: Preoperative pleural adhesion assessments included dynamic-ventilation CT of 42 smokers (including 22 patients with COPD) in the lateral position, with the unoperated lung beneath (dependent lung). The scanned lungs' mean lung density (MLD) and the bilateral main bronchi's luminal areas (Ai) were measured automatically (13–18 continuous image frames, 0.35 seconds/frame). Calculations included cross-correlation coefficients (CCCs) between the MLD and Ai time curves, and correlations between the quantitative measurements and spirometric values were evaluated by using Spearman's rank coefficient.

Results: The $\Delta MLD_{1.05}$ (from the peak inspiration frame to the third expiratory frame, 1.05 seconds later) in the nondependent lung negatively correlated with FEV_1/FVC ($r=-0.417$, $P<0.01$), suggesting that large expiratory movement of the nondependent lung would compensate limited expiratory movement of the dependent lung due to COPD. The $\Delta Ai_{1.05}$ negatively correlated with the FEV_1/FVC predicted in both the lungs ($r=-0.465$ and -0.311, $P<0.05$), suggesting that early expiratory collapses of the main bronchi indicate severe airflow limitation. The CCC correlated with FEV_1/FVC in the dependent lung ($r=-0.474$, $P<0.01$), suggesting that reduced synchrony between the proximal airway and lung occurs in patients with severe airflow limitation.

Conclusion: In COPD patients, in the lateral position, the following abnormal dynamic-ventilation CT findings are associated with airflow limitation: enhanced complementary ventilation in the nondependent lung, early expiratory airway collapses, and reduced synchrony between airway and lung movements in the dependent lung.

Keywords: COPD, computed tomography, dynamic-ventilation CT, main bronchus, mean lung density

Introduction

Recently, multiple researchers have focused on lung and thoracic movements visualized by continuous scanning by using a 320-row computed tomography (CT) scanner with 160-mm coverage.[1–5] By applying an iterative reconstruction algorithm, it has been demonstrated that ultra-low-dose (ULD) CT (0.16–0.29 mSv) has similar diagnostic capability to low-dose CT (0.92–1.74 mSv) in the field of lung cancer (nodule) screening.[6–10] These ULD settings have gradually been applied to four-dimensional (4D) dynamic-ventilation CT, which enables the observation of a longer respiratory

cycle with acceptable radiation exposure (~2.4 mSv) for the evaluation of direct invasion by lung tumors into adjacent structures and localized pleural adhesion.[11,12]

It has already been reported that an airway point can be tracked and automatically measured using a commercially available software.[13] Furthermore, mean lung density (MLD) values at each image frame of a dynamic-ventilation CT scan can be measured, although the scanned area does not always include the whole lung.[14] Among variable quantitative CT indices, airway luminal area (Ai) and MLD have been shown to be useful for the prediction of airway flow limitation severity in COPD.[15–18] In addition, based on a strong positive association between MLD and lung volume (LV),[15,19] changes in MLD values can be a surrogate for changes in LV on the dynamic-ventilation CT. By analyzing dynamic-ventilation CT images using these quantitative parameters, a new perspective for airway and lung movements has been recognized: the synchrony between proximal airway Ai and MLD values, which is limited and correlated with airflow limitation in COPD.[14] This phenomenon may reflect abnormal proximal tracheal/bronchial collapse in association with rapid tension loss in the surrounding structures during early expiration, which is followed by delayed and restricted ventilation in patients with COPD. However, as these previous studies utilized 4D CT data in the supine position only, the effects of gravity or body position on airway/lung movements remain unclear.

The effect of gravity and body position on ventilation has been investigated using apparent diffusion coefficient (ADC) values measured by hyperpolarized [3]He MRI, which can be a useful indicator of inflation level.[20] Based on the observation, ADC values are similar in nondependent (upside) and dependent (downside) regions at volumes of 100% of vital capacity (VC), whereas the dependent–nondependent vertical gradient in ADC values is observed at VC volumes of both 20% and 60% in nonsmokers, indicating that predominant ventilation occurs in the dorsal regions in the supine position.[20] Based on the observation, a change in body posture from supine to lateral/prone positions must make a great influence on ventilation and perfusion during the whole respiration in the lung field. With patients in the lateral position, ventilation is also regarded as predominant in the dependent lung in a physiological state, compared with the nondependent lung.[21] To the best of our knowledge, no previous information on continuous measurements of MLD or Ai of patients in the lateral position has been reported. Based on our observation of dynamic-ventilation CT image, strange airway/lung movements may appear, and impairment in the synchrony

between proximal airway and lung movements may occur in the lateral position.

Thus, the purpose of this study was to measure continuous changes in Ai of the proximal airways and MLD using dynamic-ventilation CT with patients in the lateral position and to assess their correlations with spirometric values.

Materials and methods

The Institutional Review Board of the Shiga University of Medical Science approved this study. Written informed consent was obtained from all the enrolled patients. This retrospective study was planned as a supplementary analysis after our previous research, which aimed at evaluating the potential of dynamic-ventilation CT for the preoperative detection of pleural adhesion.[12] All scan data were anonymized and stored in a research computer. This study was also arranged as part of the Area-Detector Computed Tomography for the Investigation of Thoracic Diseases (ACTIve) study, an ongoing multicenter research project in Japan.

Patient population

Among 85 consecutive patients who underwent dynamic-ventilation CT within a week prior to lung surgery between November 2015 and November 2016 and had no or slight pleural adhesions confirmed at surgery, 33 patients were excluded as some part of the main bronchi was located outside of the scanning area. Ten nonsmokers were also excluded because the influence of airflow limitation on lung movement for smokers in the lateral position was focused on in this study. Finally, 42 smokers with both main bronchi completely present in the scanning area were included in this study. All the enrolled subjects had resectable lung cancer or benign pulmonary lesions that were proved pathologically afterward. Among them, 22 were diagnosed with COPD. Table 1 summarizes the patient characteristics.

Dynamic-ventilation CT

Dynamic-ventilation CT was implemented after the routine preoperative protocol for CT examination. The scanning field was set in the lateral position with the unilateral affected lung field placed on the upper side (nondependent lung), mainly because of comparison in the detection performance of pleural adhesion around the targeted lung with transthoracic ultrasound at the operation.

Before the dynamic-ventilation CT, all the patients were instructed to inhale and exhale following a spoken command to give a constant respiratory rhythm, and their breathing was monitored by a radiological technologist. After each patient's breathing was confirmed visually to be synchronized with

Table 1 Patient characteristics

Characteristics	Total (n=42)	Right lateral position (n=15)	Left lateral position (n=27)	P-value[a]
Age (years)	69.8±8.4	71.4±5.8	69.3±10.0	0.673
Gender (F:M)	10:32	4:11	6:21	0.748
BMI (kg/m²)	22.5±2.6	23.8±3.8	22.2±3.3	0.217
FEV$_1$/FVC (%)	70.1±10.5	68.5±12.4	70.8±8.1	0.742
FEV$_1$ predicted (%)	90.7±15.9	86.6±18.9	94.1±11.9	0.145
Smoking index (pack-year)	42.4±28.7	57.9±30.9	36.8±25	0.181
Tumor size (mm)	21.2±15.2	21.7±15.8	21.0±15.1	0.487

Note: [a]Comparisons are estimated between the right and left lateral positions.
Abbreviation: BMI, body mass index.

the spoken command, dynamic scanning of the fixed scanning field was performed for 5.43±0.28 seconds, covering at least one respiratory cycle using a 320-row CT scanner (Aquilion ONE™, Canon Medical Systems, Otawara, Tochigi, Japan). Scanning and reconstruction parameters for the dynamic-ventilation CT were as follows: tube current, 20 mA; tube voltage, 120 kVp; rotation time, 0.35 seconds; imaging field of view, 320 mm; collimation, 0.5 mm; slice thickness, 0.5 mm; reconstruction kernel, FC13 (for mediastinum); reconstruction interval, 0.35 seconds/frame; and reconstruction method, full reconstruction. Eventually, a total of 13–18 continuous image frames were created from the scan data.

CT dose index volumes (CTDIvol) were defined based on each patient's body habitus. The effective dose was calculated by multiplying the dose-length product (DLP) values based on CTDIvol by a factor of 0.014.[22]

Image analysis: lung density measurement on dynamic-ventilation CT

Using a commercially available software (Lung Volume Measurement; Canon Medical Systems), the MLD was measured automatically in each frame, and the time curve of the MLD on the dynamic-ventilation CT scans was created. On the time curve, the peak inspiratory (minimum) MLD, peak expiratory (maximum) MLD, ΔMLD_{EI} values (defined as the subtracted value of the peak expiratory MLD from the peak inspiratory MLD divided by the peak inspiratory MLD), and the $\Delta MLD_{1.05}$ values (defined as the subtracted value of the MLD at the third frame [1.05 seconds] after the peak inspiration divided by the peak inspiratory MLD) were obtained (Figure 1).

Image analysis: quantitative airway measurement on dynamic-ventilation CT

The following procedures were performed using a commercially available research software (4D Airways Analysis; Canon Medical Systems). First, the continuous image data

(320 images/frame× total 13–18 frames, every 0.35 seconds) were synthesized for a Cine-CT series. Second, a tree of the centerlines was created automatically from the trachea to all traceable peripheral bronchi throughout the Cine-CT, on which the anatomical information of the measurement point was sustained and reproduced in each frame. Third, once the operator set a measurement point on the airway centerline in a single frame, the corresponding measurement points in other frames were determined simultaneously (Figure 2).
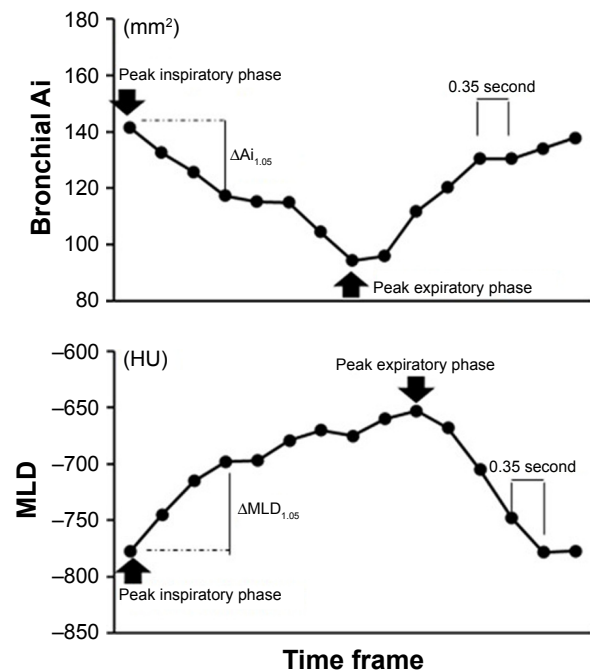

Figure 1 Example of continuous measurements of MLD and Ai in the dependent lung field.
Notes: Both MLD and Ai values are plotted in each of the 15 frames (0.35 seconds/frame). In this patient, the peak inspiratory Ai is 146.1 mm², and the peak expiratory Ai is 94.3 mm². The $\Delta Ai_{1.05}$ value is 16.5% (24.2 mm²/146.1 mm²), which was calculated between the peak inspiratory frame and the third frame after (1.05 seconds later) and adjusted by the peak inspiratory Ai as an Ai change in the early expiratory phase. The peak inspiratory MLD is −777 HU, and the peak expiratory MLD is −653 HU. The $\Delta MLD_{1.05}$ value is 10.2% (−79 HU/−777 HU), which was calculated between the peak inspiratory frame and the third frame after (1.05 seconds later) and adjusted by the peak inspiratory MLD as a density change in the early expiratory phase.
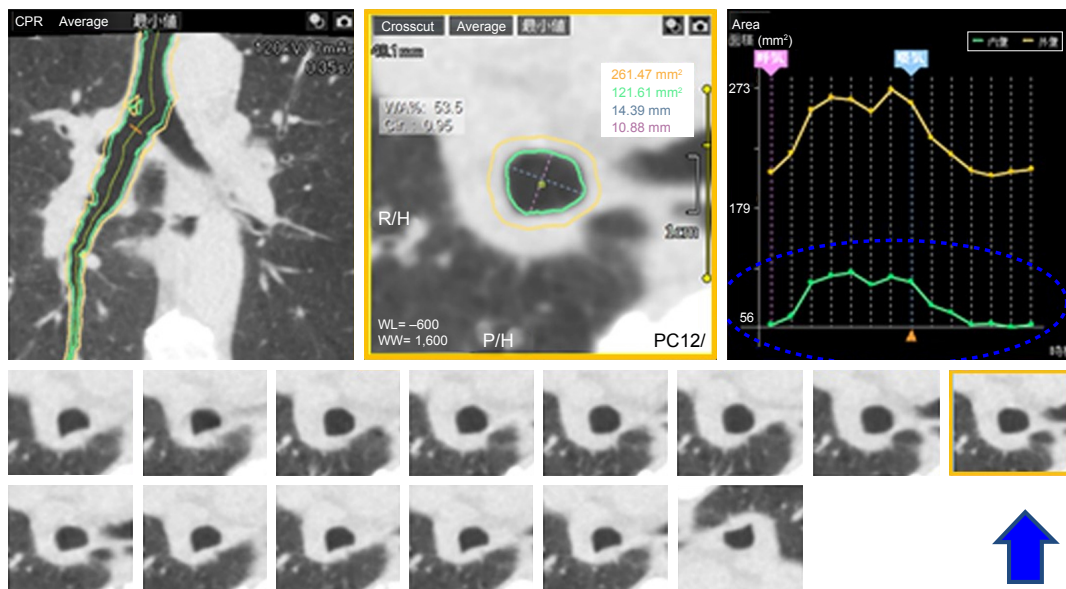**Abbreviations:** Ai, luminal area; MLD, mean lung density.

Figure 2 Example image of continuous airway measurement using the "4D Airways Analysis" software.
Notes: The corresponding measurement points in all 14 frames are shown at the bottom. On this image, a measurement point is set in the right main bronchus in the dependent lung field. A measured Ai of frame No. 8 (blue arrow) is shown in the center square (surrounded by a orange rectangle). Continuous changes in Ai are shown in the upper right square (blue dashed oval).
Abbreviation: Ai, luminal area.

Airway Ai was measured continuously at a single point of the main bronchi of both the nondependent and dependent lungs. An operator (YN, 17 years' experience in thoracic radiology) selected the middle point of each bronchus in each frame, and the time curve of the Ai on the dynamic-ventilation CT scans was created. On the time curve, the peak inspiratory (maximum) Ai, peak expiratory (minimum) Ai, ΔAi_{EI} values (defined as the subtracted value of the peak expiratory Ai from the peak inspiratory Ai divided by the peak inspiratory Ai), and the $\Delta Ai_{1.05}$ values (defined as the subtracted value of the Ai at the third frame [1.05 seconds] after the peak inspiration divided by the peak inspiratory Ai) were obtained (Figure 1).

Spirometric evaluation
Within 1 month of the dynamic-ventilation CT date, all the patients underwent spirometry, including FEV_1 and FVC, in accordance with the American Thoracic Society standards.[23]

Statistical analyses
Cross-correlation coefficients (CCC; $-1<R<1$) were calculated between the time curves of the MLD and airway Ai of the main bronchus. If the two time curves were completely opposite in direction over time, the coefficient

approached -1. Spearman's rank correlation analyses were performed to assess the associations of the CT indices with the FEV_1/FVC, the FEV_1 predicted, and a cumulative smoking index. Correlations were compared using the Meng–Rosenthal–Rubin method with Fisher's r-to-z transformation.[24] Measured values for the MLD and Ai were compared between the nondependent and dependent lung fields, between peak inspiration and peak expiration, and between the right and left lateral positions at the peak inspiration, in each of the nondependent and dependent lung fields. A P-value of 0.05 was considered significant. All statistical analyses were performed using SPSS software Version 22 (IBM Corporation, Chicago, IL, USA).

Results
Patient characteristics
Table 1 summarizes the characteristics of the enrolled patients, including spirometric values. There were no significant differences between two patient groups of the right and left lateral positions (Table 1).

Radiation dose assessment for dynamic-ventilation CT
For a single gantry rotation of 160 mm (0.35 seconds), the CTDIvol was 0.504 mGy. The DLP value for a single rotation

was 8.06 mGy·cm. The total estimated radiation exposure for dynamic-ventilation CT for 4.55–6.3 seconds varied from 1.78 to 2.46 mSv (2.12±0.11 mSv).

Dynamic MLD measurements

MLD at end expiration was higher than that at end inspiration in both the dependent and nondependent lung fields ($P<0.001$). During a respiratory cycle, the MLD changed by the mean values of 88.5 and 32.4 HU in the dependent and nondependent lungs, respectively. MLD at peak expiration in the nondependent lung field was lower than that in the dependent lung field ($P<0.001$). Both ΔMLD_{EI} and $\Delta MLD_{1.05}$ in the dependent lung field were larger than those in the nondependent lung field ($P<0.001$). At the peak inspiration, MLD in the dependent lung (right: −809.7±32.4 vs left: −812.3±30.8; $P=0.646$) and that in the nondependent lung (right: −849.8±33.4 vs left: −851.5±19.6; $P=0.703$) were similar between the right and left lateral position. The $\Delta MLD_{1.05}$ did not correlate with FEV_1/FVC in the dependent lung but did negatively correlate with FEV_1/FVC in the nondependent lung ($r=−0.417$, $P=0.006$). The nondependent/dependent ratio of the $\Delta MLD_{1.05}$ also showed a negative correlation with FEV_1/FVC ($r=−0.476$, $P=0.001$). ΔMLD_{EI} also correlated with FEV_1/FVC in the nondependent lung ($r=−0.344$, $P=0.026$); however, its correlation was weaker compared with that between $\Delta MLD_{1.05}$ and FEV_1/FVC. In the dependent lung, peak inspiratory MLD had a mild positive correlation with FEV_1/FVC ($r=0.448$, $P=0.003$), whereas in the nondependent lung neither peak inspiratory nor expiratory MLD correlated with FEV_1/FVC or FEV_1 predicted (Table 2).

Dynamic bronchial Ai measurements

In total, 1,310 middle points of the main bronchi were analyzed for Ai measurements. Among them, 255 points (19.5%) were minimally modified by the operator. Ai at the peak inspiration was smaller than that at the peak expiration in both the dependent and nondependent lungs. Ai at the peak inspiration in the nondependent lung field was larger than that in the dependent lung field ($P=0.019$). Both ΔAi_{EI} and $\Delta Ai_{1.05}$ in the dependent lung field were larger than those in the nondependent lung field ($P<0.001$). At the peak inspiration, right Ai (154.0±50.6) was larger than left Ai (117.1±38.6) in the dependent lung ($P=0.001$), and right Ai (165.6±52.0) was larger than left Ai (136.8±54.3) in the nondependent lung ($P=0.002$). The mean ΔAi_{EI} values of the main bronchi were 18.5% in the dependent lung and 10.5% in the nondependent lung. In the nondependent lung, both ΔAi_{EI} and $\Delta Ai_{1.05}$ correlated with FEV_1/FVC ($r=−0.431$, $P=0.004$; $r=−0.465$, $P=0.002$). In the dependent lung, ΔAi_{EI} did not show any correlation with FEV_1/FVC ($r=−0.232$, $P=0.140$), whereas $\Delta Ai_{1.05}$ showed a negative correlation with FEV_1/FVC ($r=−0.311$, $P=0.045$; Figures 3 and 4). These data indicate that the early expiratory collapses of the main bronchi are associated with airflow limitation in COPD (Table 3).

Table 2 Lung density measurements and correlations to clinical indices

	Measured value	Correlation to FEV_1/FVC	Correlation to FEV_1 predicted	Correlation to smoking index
	Mean±SD (range)	r (P-value)	r (P-value)	r (P-value)
Nondependent lung				
End-inspiratory MLD (HU)	−850.9±24.0 ([−930]–[−804])	0.272 (0.082)	−0.074 (0.640)	0.036 (0.822)
End-expiratory MLD (HU)	−818.5±35.3 ([−909]–[−700])	0.031 (0.844)	−0.046 (0.774)	0.023 (0.885)
ΔMLD_{EI} (%)	3.8±2.2 (0.2–13.6)	−0.344 (0.026[a])	−0.036 (0.822)	−0.07 (0.661)
$\Delta MLD_{1.05}$ (%)	1.9±1.1 (0.1–5.1)	−0.417 (0.006[a])	−0.089 (0.574)	−0.023 (0.885)
%LAA$_{-950}$ at end inspiration	6.5±11.1 (0.0–61.1)	−0.552 (<0.001[a])	−0.103 (0.517)	0.130 (0.414)
Dependent lung				
End-inspiratory MLD (HU)	−811.3±31.0 ([−877]–[−740])	0.448 (0.003[a])	0.010 (0.948)	−0.042 (0.790)
End-expiratory MLD (HU)	−723.4±45.2 ([−819]–[−628])	0.254 (0.104)	0.166 (0.293)	−0.017 (0.915)
ΔMLD_{EI} (%)	10.9±3.8 (2.2–18.5)	0.043 (0.785)	0.242 (0.123)	−0.039 (0.804)
$\Delta MLD_{1.05}$ (%)	6.1±2.7 (1.9–14.1)	−0.056 (0.723)	0.122 (0.442)	0.137 (0.387)
%LAA$_{-950}$ at end inspiration	3.3±7.0 (0–32.7)	−0.551 (<0.001[a])	−0.148 (0.351)	0.007 (0.963)
Nondependent/dependent ratio in $\Delta MLD_{1.05}$	0.31±0.19 (0.06–1.01)	−0.476 (0.001[a])	−0.293 (0.060)	0.163 (0.313)

Note: [a]Significant.

Abbreviations: MLD, mean lung density; ΔMLD_{EI}, the subtracted value of the peak expiratory MLD from the peak inspiratory MLD divided by the peak inspiratory MLD; $\Delta MLD_{1.05}$, the subtracted value of the MLD at the third frame (1.05 seconds) after the peak inspiration divided by the peak inspiratory MLD; %LAA$_{-950}$, the ratio of low attenuation area (under −950 HU) to the total lung field; HU, Hounsfield unit.
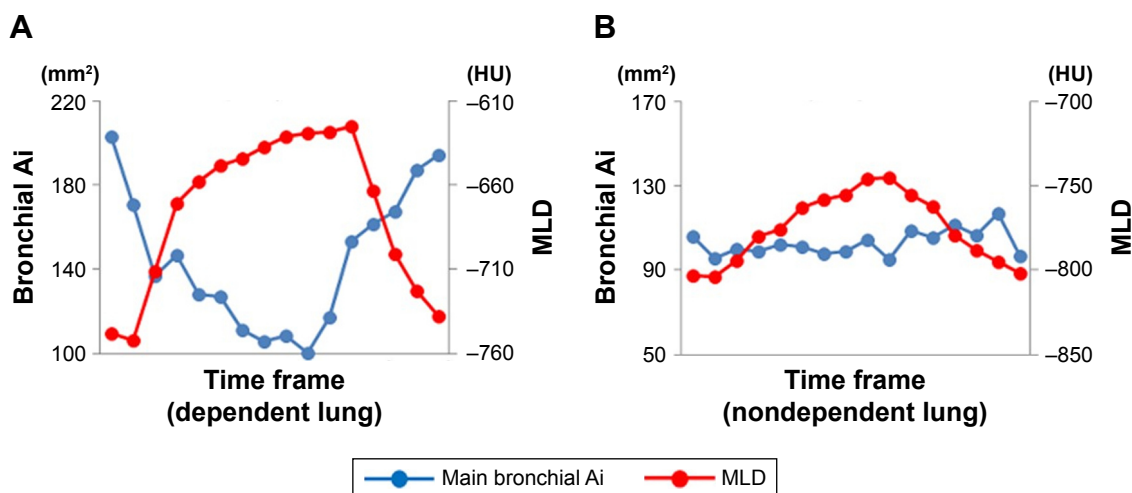
Figure 3 Measurements of cross-correlation coefficients between the two time curves from the MLD and the airway Ai in the dependent lung (**A**) and nondependent lung (**B**) of a male smoker without COPD ($FEV_1/FVC=0.70$).
Notes: The two time curves of the MLD and the main bronchial Ai movement in the right dependent lung are in almost opposite directions, suggesting that the tracheal dilation and the lung inflation occurred simultaneously. The cross-correlation coefficient between the two time curves was large and negative (−0.84) (**A**). The two time curves of the MLD and the main bronchial Ai movement in the left nondependent lung moved independently of each other (cross-correlation coefficient=−0.14) (**B**). Change in the main bronchial Ai in the left nondependent lung (**B**) was much smaller than that in the right dependent lung (**A**). The nondependent/dependent ratio in the $\Delta MLD_{1.05}$ value was 0.264.
Abbreviations: Ai, luminal area; MLD, mean lung density; HU, Hounsfield unit.

Relationship between MLD and main bronchial Ai

In the nondependent lung, the $\Delta MLD_{1.05}$ correlated positively with the $\Delta Ai_{1.05}$ ($r=0.465$, $P=0.002$), whereas in the dependent lung field the $\Delta MLD_{1.05}$ did not correlate with the $\Delta Ai_{1.05}$ ($r=0.243$, $P=0.122$).

In the dependent lung, the CCC between the main bronchial Ai and MLD correlated with the FEV_1/FVC ($r=-0.474$,

$P=0.002$), whereas in the nondependent lung no significant association was found between the CCC and airflow limitation. These findings suggested that the synchrony between the airway and lung movements was attenuated in association with the degree in the airflow limitation in the dependent lung only (Table 4; Figures 3–5; Videos S1 and S2). The CCC in the dependent lung had associations with FEV_1/FVC in both the right lateral position ($r=-0.657$, $P=0.008$) and the
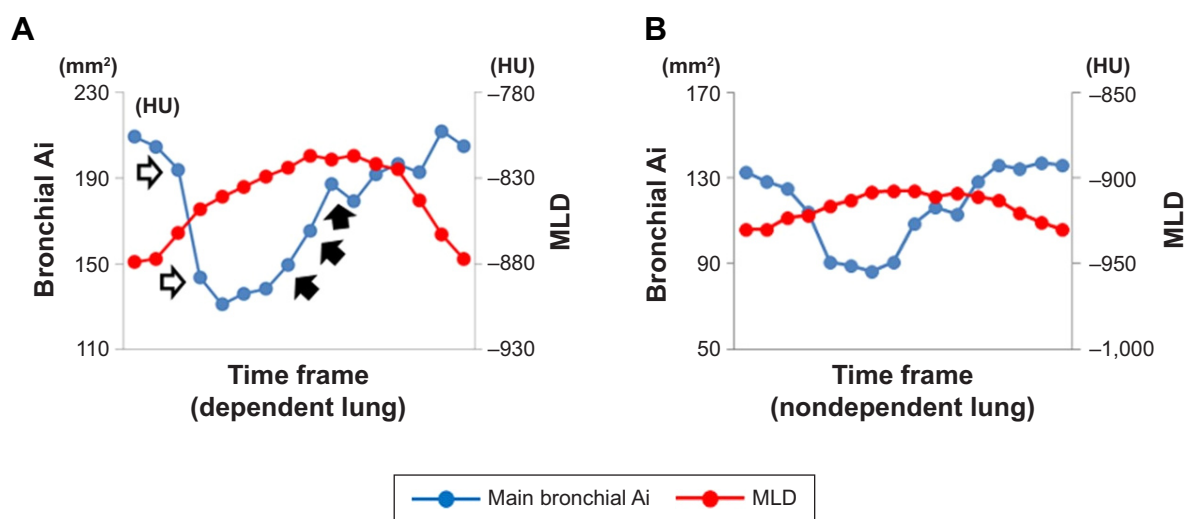

Figure 4 Measurements of cross-correlation coefficients between the two time curves from the MLD and the airway Ai in the dependent lung (**A**) and nondependent lung (**B**) of a male smoker with COPD ($FEV_1/FVC=0.544$).
Notes: It was unclear that the two time curves of the MLD and the main bronchial Ai movement in the right dependent lung moved in opposite directions (cross-correlation coefficient=−0.46) (**A**). Furthermore, the main bronchial Ai decreased rapidly in the early expiratory phase (white arrows) followed by a strange increase during the middle-to-late-expiratory phases (black arrows), suggesting the presence of paradoxical airway movement (**A**). The two time curves of the MLD and the main bronchial Ai movement in the left nondependent lung are in relatively opposite directions (cross-correlation coefficient=−0.601) (**B**). The nondependent/dependent ratio in the $\Delta MLD_{1.05}$ value was relatively large (0.389), due to mild increase in MLD during expiration caused by COPD.
Abbreviations: Ai, luminal area; MLD, mean lung density; HU, Hounsfield unit.

Table 3 Airway dimension measurements and correlations to clinical indices

	Measured value	Correlation to FEV$_1$/FVC	Correlation to FEV$_1$ predicted	Correlation to smoking index
	Mean±SD (range)	r (P-value)	r (P-value)	r (P-value)
Nondependent main bronchus				
End-inspiratory Ai (mm^2)	148.6±51.4 (73.3–302.7)	0.004 (0.98)	−0.031 (0.847)	0.047 (0.769)
End-expiratory Ai (mm^2)	125.6±44.5 (57.5–237.6)	0.102 (0.52)	0.096 (0.547)	−0.006 (0.970)
ΔAi$_{EI}$ (%)	10.5±10.6 ([−13.7]–38.5)	−0.431 (0.004[a])	−0.300 (0.054)	0.041 (0.797)
ΔAi$_{1.05}$ (%)	6.8±7.9 ([−7.0]–30.0)	−0.465 (0.002[a])	−0.290 (0.063)	0.099 (0.535)
Dependent main bronchus				
End-inspiratory Ai (mm^2)	132.3±45.1 (66.9–273.3)	−0.050 (0.755)	−0.078 (0.623)	0.310 (0.046[a])
End-expiratory Ai (mm^2)	105.2±31.8 (41.5–166.9)	0.037 (0.817)	0.062 (0.698)	0.192 (0.224)
ΔAi$_{EI}$ (%)	18.5±10.9 ([−8.5]–44.4)	−0.232 (0.140)	−0.276 (0.077)	0.256 (0.102)
ΔAi$_{1.05}$ (%)	14.1±10.5 (1.9–44.9)	−0.311 (0.045[a])	−0.523 (<0.001[a])	0.291 (0.062)

Note: [a]Significant.
Abbreviations: Ai, luminal area; ΔAi$_{EI}$, the subtracted value of the peak expiratory Ai from the peak inspiratory Ai divided by the peak inspiratory Ai; ΔAi$_{1.05}$, the subtracted value of the Ai at the third frame (1.05 seconds) after the peak inspiration divided by the peak inspiratory Ai.

left lateral position (r=−0.400, P=0.038; Table 4). In the right lateral position, the CCC had a negative association with FEV$_1$ predicted in the dependent lung field (r=−0.545, P=0.036) and a positive association with FEV$_1$ predicted in the nondependent lung (r=0.559, P=0.030; Table 4).

Discussion

In this study, we quantitatively assessed dynamic-ventilation CT performed in the lateral position and found the following: 1) although the MLD change in the early expiratory phase (within 1.05 seconds) did not correlate with the airflow limitation in the dependent lung, that in the nondependent lung negatively correlated with the airflow limitation, suggesting that larger early expiratory movements in the nondependent lung are found in patients with more severe airflow limitation; 2) early expiratory collapse of the main bronchus was associated with airflow limitation in both the nondependent and dependent lungs, which has been reported by a few previous studies and was first demonstrated as

reproducible quantitative data; and 3) reduced synchrony in the dependent lung between the main bronchial and lung movements was associated with the severity of airflow limitation. Based on these observations, we strongly believe that continuous respiratory movements of the lung and central airways depicted by the dynamic-ventilation CT in the lateral position can bring novel insights into the pathophysiology of COPD, particularly regarding the impact of gravity and body position in ventilation.

In this study, the MLD change in the early expiratory phase in the dependent lung did not correlate with airflow limitation. This result seems to be discordant with the excellent positive correlation in the supine position.[14] In addition, as MLD is considered to be a good predictor of airflow limitation and air trapping on static CT scans[18,25–28] and the changes in MLD in respiratory cycles can be considered as changes in LV,[14,19] the insignificant correlations between the MLD changes in the early expiratory phase and spirometric parameters seem to be strange. This phenomenon may be attributable to

Table 4 CCCs (between main bronchial Ai and MLD) and correlations to clinical indices

	CCC between airway Ai and MLD	Correlation to FEV$_1$/FVC	Correlation to FEV$_1$ predicted	Correlation to smoking index
	Mean±SD (range)	r (P-value)	r (P-value)	r (P-value)
Total (n=42)				
Nondependent main bronchus	[−0.581]±0.389 ([−0.951]–0.451)	0.229 (0.145)	0.024 (0.882)	0.006 (0.97)
Dependent main bronchus	[−0.721]±0.162 ([−0.912]–[−0.258])	−0.474 (0.002[a])	−0.232 (0.139)	0.183 (0.246)
Right lateral position (n=15)				
Nondependent main bronchus	[−0.567]±0.353 ([−0.904]–0.451)	0.279 (0.315)	0.559 (0.030[a])	−0.333 (0.147)
Dependent main bronchus	[−0.712]±0.187 ([−0.857]–[−0.258])	−0.657 (0.008[a])	−0.545 (0.036[a])	0.254 (0.362)
Left lateral position (n=27)				
Nondependent main bronchus	[−0.588]±0.406 ([−0.951]–0.419)	0.230 (0.249)	−0.266 (0.18)	0.155 (0.441)
Dependent main bronchus	[−0.727]±0.147 ([−0.912]–[−0.321])	−0.400 (0.038[a])	−0.032 (0.874)	0.207 (0.3)

Note: [a]Significant.
Abbreviations: Ai, luminal area; CCC, cross-correlation coefficient; MLD, mean lung density.
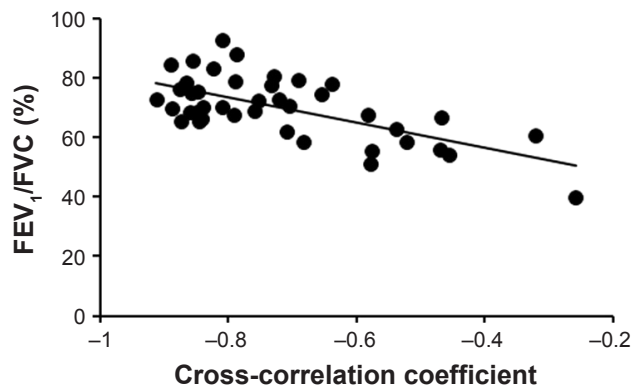
Figure 5 Scatter plots of the cross-correlation coefficient between two time curves of MLD and the main bronchial Ai movement in the dependent lung for the total study population (n=42) with FEV_1/FVC.
Abbreviations: Ai, luminal area; MLD, mean lung density.

a decrease in VC of the dependent lung in the lateral position, which can be associated with the mediastinum located upward, compared with the supine or prone positions, or to the presumed physiological difference between the unilateral dependent lung in the lateral position and the bilateral lungs in the sitting position for spirometry. Interestingly, in the nondependent lung, the increase in MLD in the early expiratory phase negatively correlated with FEV_1/FVC, suggesting that the proximal airway closure is delayed in COPD to obtain larger expiratory lung movements. This was also supported by the nondependent/dependent ratio of MLD change in the early-expiratory phase, which was larger in patients with more severe airflow limitation. In addition, the MLD change in the total expiratory phase also correlated negatively with FEV_1/FVC. These observations suggest the existence of complementary ventilation in the nondependent lung, which would appear to compensate insufficient ventilation in the dependent lung in patients with COPD to some extent. This indicates that the less affected lung may be placed uppermost in COPD patients in the lateral position to improve ventilation in part when the patient has large atelectasis or pneumonia. If this result is validated by other large study populations in the future, this knowledge would also be applicable to pulmonary rehabilitation in the lateral position and important for better understanding of the pathogenesis of COPD.

Another interesting finding of the current study is that the changes in the main bronchial Ai in the early expiratory phase negatively correlated with FEV_1 predicted in the nondependent and dependent lungs. Moreover, these correlations were stronger compared with ΔAi_{EI} from the total expiratory phase. The meaning of highly collapsed proximal airways observed on conventional CT in COPD patients

still remains unclear and controversial.[29–35] For instance, while the collapsed trachea in the well-collapsed lung on (static) expiratory CT often indicates good lung function,[34,35] the expiratory/inspiratory ratio of middle-sized bronchial Ai positively correlates with airflow limitation.[17] These inconsistent results may be due to differences in respiration levels corresponding to the "suspected" end-expiratory phase. In fact, for the assessment of lobar air trapping, MLD changes from end inspiration to end expiration corrected with the LV decrease were reported to be important.[36] Compared with the previous reports using static inspiratory and expiratory CT scans, the abnormal collapse of the proximal airway during early expiration on dynamic-ventilation CT was first correlated with the airflow limitation in this study. The rapid decrease in proximal bronchial Ai during early expiration detected on dynamic-ventilation CT may be a new indicator for COPD severity. This collapse of the proximal bronchi in COPD would cause a delay in expiration in the peripheral bronchi and result in time lags in the movement among different pulmonary regions. Such early expiratory collapse of the proximal bronchi may be a target for future therapeutic strategies for COPD.

In the dependent lung in the lateral position, reduced synchrony between the main bronchial and lung movements was associated with airflow limitation, which was compatible with the results of a previous study analyzing bilateral lung fields using dynamic-ventilation CT in the supine position.[14] In addition, ΔMLD_{EI} in the dependent lung was demonstrated to be larger as compared with the nondependent lung. In the lateral position, it was demonstrated that gravity affects ventilation–perfusion matching, which is independent from the hypoxic pulmonary vasoconstrictive response.[37–39] In a previous study addressing the role of gravity in the vascular flow redistribution in the lung during one-lung ventilation for COPD patients, the partial pressure of arterial oxygen during one-lung ventilation in the dependent lung in the lateral position decreased by only about 10% compared with bilateral lung ventilation in the supine position.[38] Although the association of the synchrony between the main bronchial and lung movements with ventilation–perfusion relationship has not been evaluated, reduced synchrony in COPD may lead to partial ventilation–perfusion imbalance in the dependent lung field and generate complementary lung movement in the nondependent lung. We speculate that a similar phenomenon might be found in the dorsal region in the lower lung field in the supine position, and disconnection between airway and lung movements would prevent effective gas exchange in the lung.

At the end inspiration, more Ai reduction in the dependent lung based on the nondependent lung for the left main bronchus (117.1±38.6 in the dependent and 136.8±54.3 in the nondependent lungs) was observed as compared with the right main bronchus (154.0±50.6 in the dependent and 165.6±52.0 in the nondependent lungs).

Considering the positional relationship between the heart and main bronchus, this result may be probably due to more compression and direct pulsation effects of the heart to the main bronchus in the left dependent lung field. Therefore, in the left lateral position, CCC between the main bronchial Ai and MLD at the left lateral position may be attenuated in the dependent lung field, and complimentary ventilation may occur in the nondependent lung field even for some smokers without airflow limitation, resulting in the attenuated correlation between CCC and FEV_1/FVC or FEV_1 predicted in the nondependent and dependent lung fields. On the other hand, in the right lateral position, main bronchi in the nondependent lung field may not be affected so much by the heart, which is supported by the result that there was a positive correlation of CCC between main bronchial Ai and MLD with FEV_1 predicted. These issues relevant to the influence of the heart on the proximal bronchial and lung mechanics are crucial and should be assessed in detail in our future study.

There were several limitations in this study. First, because this study was performed as a preliminary study to evaluate the association of the synchrony in MLD and Ai with airflow limitation severity on dynamic-ventilation CT, the total number of enrolled patients was small. Thus, the results of this study should be evaluated further in a larger study population without lung tumors. Second, the scanning area could not include the whole thorax. Although we believed that it was best to substitute the MLD measurement as a surrogate for LV measurement, actual respiratory changes in LV could not be measured. Third, we did not measure the trachea and more peripheral bronchi, mainly because we focused on the comparison of the proximal bronchi between the nondependent and dependent lungs. It has been widely accepted that the airway dimensions or wall thickening in the more peripheral airways has been demonstrated to reflect airflow limitation more precisely. Improvement in the software will enable us to measure more peripheral airways on the dynamic-ventilation CT. Fourth, extra radiation exposure for the dynamic-ventilation CT (~2.1 mSv in this study) may lead to concerns about the application of this method in routine clinical examinations. Although the tube current was fixed at 20 mA in this study, a reduced tube current, such as 10 mA,

may be feasible in future studies, particularly in combination with more powerful iterative reconstruction techniques. Fifth, the influence of dose reduction on lung densitometry could not be an ignorable issue in this study. However, in a previous study, MLD measured on chest CT image at considerably reduced dose (10 mA) was demonstrated to be almost equivalent to that at standard dose (240 mA) in identical cases.[40] Therefore, considering the tube current adopted in dynamic-ventilation CT was 20 mA, measurement errors in the lung densitometry are thought to be actually too small to bring a crucial problem to our evaluation. Sixth, the severity of airflow limitation in most of the COPD patients was mild (FEV_1 predicted >80%). Whether or not similar results are obtained in patients with severe degree of COPD is unknown and should be examined in a future study for larger study population of patients with more severe airflow limitation.

Conclusion

In conclusion, dynamic-ventilation CT in the lateral position demonstrated that airflow limitation was associated with reduced synchrony between the proximal airway and lung movement in the dependent lung and enhanced complimentary ventilation in the nondependent lung, in addition to early expiratory, pathological, proximal airway collapse in both the lungs.

Disclosure

References

1. Lee EY, Zucker EJ, Restrepo R, Daltro P, Boiselle PM. Advanced large airway CT imaging in children: evolution from axial to 4-D assessment. *Pediatr Radiol*. 2013;43(3):285–297.
2. Choong CK, Pasricha SS, Li X, et al. Dynamic four-dimensional computed tomography for preoperative assessment of lung cancer invasion into adjacent structures. *Eur J Cardiothorac Surg*. 2015;47(2):239–243.
3. Troupis JM, Pasricha SS, Narayanan H, Rybicki FJ, Pick AW. 4D CT and lung cancer surgical resectability: a technical innovation. *J Med Imaging Radiat Oncol*. 2014;58(4):469–471.
4. Tan JZ, Crossett M, Ditchfield M. Dynamic volumetric computed tomographic assessment of the young paediatric airway: initial experience of rapid, non-invasive, four-dimensional technique. *J Med Imaging Radiat Oncol*. 2013;57(2):141–148.
5. Fujimoto R, Sato M, Miyata R, et al. Successful resection of recurrent mediastinal liposarcoma using preoperative evaluation of organ invasion by four-dimensional computed tomography. *Gen Thorac Cardiovasc Surg*. 2016;64(8):488–491.
6. Nagatani Y, Takahashi M, Murata K, et al. Lung nodule detection performance in five observers on computed tomography (CT) with adaptive iterative dose reduction using three-dimensional processing (AIDR 3D) in a Japanese multicenter study: comparison between ultra-low-dose CT and low-dose CT by receiver-operating characteristic analysis. *Eur J Radiol*. 2015;84(7):1401–1412.
7. Neroladaki A, Botsikas D, Boudabbous S, Becker CD, Montet X. Computed tomography of the chest with model-based iterative reconstruction using a radiation exposure similar to chest X-ray examination: preliminary observations. *Eur Radiol*. 2013;23(2):360–366.
8. Nagatani Y, Takahashi M, Ikeda M, et al. Sub-solid nodule detection performance on reduced-dose computed tomography with iterative reduction: comparison between 20 mA (7 mAs) and 120 mA (42 mAs) regarding nodular size and characteristics and association with size-specific dose estimate. *Acad Radiol*. 2017;24(8):995–1007.
9. Katsura M, Matsuda I, Akahane M, et al. Model-based iterative reconstruction technique for ultralow-dose chest CT: comparison of pulmonary nodule detectability with the adaptive statistical iterative reconstruction technique. *Invest Radiol*. 2013;48(4):206–212.
10. Nagatani Y, Moriya H, Noma S, et al. Association of focal radiation dose adjusted on cross sections with subsolid nodule visibility and quantification on computed tomography images using AIDR 3D: comparison among scanning at 84, 42, and 7 mAs. *Acad Radiol*. 2018;25(9):1156–1166.
11. Sakuma K, Yamashiro T, Moriya H, Murayama S, Ito H. Parietal pleural invasion/adhesion of subpleural lung cancer: quantitative 4-dimensional CT analysis using dynamic-ventilatory scanning. *Eur J Radiol*. 2017;87:36–44.
12. Hashimoto M, Nagatani Y, Oshio Y, et al. Preoperative assessment of pleural adhesion by four-dimensional ultra-low-dose computed tomography (4D-ULDCT) with adaptive iterative dose reduction using three-dimensional processing (AIDR-3D). *Eur J Radiol*. 2018;98(1):179–186.
13. Yamashiro T, Tsubakimoto M, Nagatani Y, et al. Automated continuous quantitative measurement of proximal airways on dynamic ventilation CT: initial experience using an ex vivo porcine lung phantom. *Int J Chron Obstruct Pulmon Dis*. 2015;10(1):2045–2054.
14. Yamashiro T, Moriya H, Tsubakimoto M, Matsuoka S, Murayama S. Continuous quantitative measurement of the proximal airway dimensions and lung density on four-dimensional dynamic-ventilation CT in smokers. *Int J Chron Obstruct Pulmon Dis*. 2016;11(1):755–764.
15. Kundu S, Gu S, Leader JK, et al. Assessment of lung volume collapsibility in chronic obstructive lung disease patients using CT. *Eur Radiol*. 2013;23(6):1564–1572.
16. Hasegawa M, Nasuhara Y, Onodera Y, et al. Airflow limitation and airway dimensions in chronic obstructive pulmonary disease. *Am J Respir Crit Care Med*. 2006;173(12):1309–1315.
17. Matsuoka S, Kurihara Y, Yagihashi K, Hoshino M, Nakajima Y. Airway dimensions at inspiratory and expiratory multisection CT in chronic obstructive pulmonary disease: correlation with airflow limitation. *Radiology*. 2008;248(3):1042–1049.
18. Camiciottoli G, Cavigli E, Grassi L, et al. Prevalence and correlates of pulmonary emphysema in smokers and former smokers. A densitometric study of participants in the ITALUNG trial. *Eur Radiol*. 2009;19(1):58–66.
19. Yamashiro T, Matsuoka S, Bartholmai BJ, et al. Collapsibility of lung volume by paired inspiratory and expiratory CT scans: correlations with lung function and mean lung density. *Acad Radiol*. 2010;17(4):489–495.
20. Halaweish AF, Hoffman EA, Thedens DR, Fuld MK, Sieren JP, van Beek EJ. Effect of lung inflation level on hyperpolarized 3He apparent diffusion coefficient measurements in never-smokers. *Radiology*. 2013;268(2):572–580.
21. Krieg S, Alison JA, Mccarren B, Cowell S. Position affects distribution of ventilation in the lungs of older people: an experimental study. *Aust J Physiother*. 2007;53(3):179–184.
22. Shrimpton PC, Hillier MC, Lewis MA, Dunn M. National survey of doses from CT in the UK: 2003. *Br J Radiol*. 2006;79(948):968–980.
23. Vestbo J, Hurd SS, Agustí AG, et al. Global strategy for the diagnosis, management, and prevention of chronic obstructive pulmonary disease: GOLD executive summary. *Am J Respir Crit Care Med*. 2013;187(4):347–365.
24. Johns BR, Abbasi F, Reaven GM. Estimates of insulin secretory function in apparently healthy volunteers vary as a function of how the relevant variables are quantified. *Clin Chem*. 2011;57(4):627–632.
25. Lee YK, Oh YM, Lee JH, et al. Quantitative assessment of emphysema, air trapping, and airway thickening on computed tomography. *Lung*. 2008;186(3):157–165.
26. O'Donnell RA, Peebles C, Ward JA, et al. Relationship between peripheral airway dysfunction, airway obstruction, and neutrophilic inflammation in COPD. *Thorax*. 2004;59(10):837–842.
27. Kubo K, Eda S, Yamamoto H, et al. Expiratory and inspiratory chest computed tomography and pulmonary function tests in cigarette smokers. *Eur Respir J*. 1999;13(2):252–256.
28. Kundu S, Gu S, Leader JK, et al. Assessment of lung volume collapsibility in chronic obstructive lung disease patients using CT. *Eur Radiol*. 2013;23(6):1564–1572.
29. Boiselle PM, O'Donnell CR, Bankier AA, et al. Tracheal collapsibility in healthy volunteers during forced expiration: assessment with multidetector CT. *Radiology*. 2009;252(1):255–262.
30. Ederle JR, Heussel CP, Hast J, et al. Evaluation of changes in central airway dimensions, lung area and mean lung density at paired inspiratory/expiratory high-resolution computed tomography. *Eur Radiol*. 2003;13(11):2454–2461.
31. Ochs RA, Petkovska I, Kim HJ, Abtin F, Brown M, Goldin J. Prevalence of tracheal collapse in an emphysema cohort as measured with end-expiration CT. *Acad Radiol*. 2009;16(1):46–53.
32. Thiriet M, Maarek JM, Chartrand DA, et al. Transverse images of the human thoracic trachea during forced expiration. *J Appl Physiol*. 1989;67(3):1032–1040.
33. Sverzellati N, Rastelli A, Chetta A, et al. Airway malacia in chronic obstructive pulmonary disease: prevalence, morphology and relationship with emphysema, bronchiectasis and bronchial wall thickening. *Eur Radiol*. 2009;19(7):1669–1678.
34. Camiciottoli G, Diciotti S, Bigazzi F, et al. Is intrathoracic tracheal collapsibility correlated to clinical phenotypes and sex in patients with COPD? *Int J Chron Obstruct Pulmon Dis*. 2015;10:843–852.

35. Yamashiro T, San José Estépar R, Matsuoka S, et al. Intrathoracic tracheal volume and collapsibility on inspiratory and end-expiratory CT scans correlations with lung volume and pulmonary function in 85 smokers. *Acad Radiol*. 2011;18(3):299–305.

36. Nagatani Y, Murata K, Takahashi M, et al. A new quantitative index of lobar air trapping in chronic obstructive pulmonary disease (COPD): comparison with conventional methods. *Eur J Radiol*. 2015;84(5): 963–974.

37. Szegedi LL, D'Hollander AA, Vermassen FE, Deryck F, Wouters PF. Gravity is an important determinant of oxygenation during one-lung ventilation. *Acta Anaesthesiol Scand*. 2010;54(6):744–750.

38. Bardoczky GI, Szegedi LL, D'Hollander AA, Moures JM, de Francquen P, Yernault JC. Two-lung and one-lung ventilation in patients with chronic obstructive pulmonary disease: the effects of position and F(IO)2. *Anesth Analg*. 2000;90(1):35–41.

39. Arborelius M, Lundin G, Svanberg L, Defares JG. Influence of unilateral hypoxia on blood flow through the lungs in man in lateral position. *J Appl physiol*. 1960;15:595–597.

40. Nishio M, Koyama H, Ohno Y, et al. Emphysema quantification using ultralow-dose CT with iterative reconstruction and filtered back projection. *AJR Am J Roentgenol*. 2016;206(6):1184–1192.

Supplementary materials

Video S1 The dynamic-ventilation computed tomography of a non-COPD smoker. It is clear that the dependent (downside) right lung mainly respires, comparing with the nondependent (upside) left lung.

Video S2 The dynamic-ventilation computed tomography of a COPD patient. The dependent (downside) right lung and nondependent (upside) left lung move similarly, suggesting that the nondependent lung respires largely comparing with the non-COPD smoker in Video 1.